

# A Histone H3 Lysine 36 Trimethyltransferase Links Nkx2-5 to Wolf-Hirschhorn Syndrome

Paper in journals : this is the first page of a paper published in *Nature*.

[*Nature*] 460, 287-291 (2009)

Vol 460 | 9 July 2009 | doi:10.1038/nature08086

nature

## LETTERS

### A histone H3 lysine 36 trimethyltransferase links Nkx2-5 to Wolf-Hirschhorn syndrome

Keisuke Nimura<sup>1</sup>, Kiyoe Ura<sup>1</sup>, Hidetaka Shiratori<sup>2</sup>, Masato Ikawa<sup>3</sup>, Masaru Okabe<sup>3</sup>, Robert J. Schwartz<sup>4</sup> & Yasufumi Kaneda<sup>1</sup>

Diverse histone modifications are catalysed and recognized by various specific proteins, establishing unique modification patterns that act as transcription signals<sup>1,2</sup>. In particular, histone H3 trimethylation at lysine 36 (H3K36me3) is associated with actively transcribed regions and has been proposed to provide landmarks for continuing transcription<sup>3,4</sup>; however, the control mechanisms and functions of H3K36me3 in higher eukaryotes are unknown. Here we show that the H3K36me3-specific histone methyltransferase (HMTase) Wolf-Hirschhorn syndrome candidate 1 (WHSC1, also known as NSD2 or MMSET) functions in transcriptional regulation together with developmental transcription factors whose defects overlap with the human disease Wolf-Hirschhorn syndrome (WHS)<sup>5,6</sup>. We found that mouse Whsc1, one of five putative Set2 homologues<sup>7,8</sup>, governed H3K36me3 along euchromatin by associating with the cell-type-specific transcription factors Sall1, Sall4 and Nanog in embryonic stem cells, and Nkx2-5 in embryonic hearts, regulating the expression of their target genes. Whsc1-deficient mice showed growth retardation and various WHS-like midline defects, including congenital cardiovascular anomalies. The effects of Whsc1 haploinsufficiency were increased in Nkx2-5 heterozygous mutant hearts, indicating their functional link. We propose that WHSC1 functions together with developmental transcription factors to prevent the inappropriate transcription that can lead to various pathophysiologicals.

Deletions of human chromosome 4p16.3 cause the dominant disorder WHS, which is characterized by cranio-facial malformations, learning disability, growth delays, heart defects and a diverse array of associated problems, many of which can be characterized as midline defects<sup>9,6</sup>. The considerable variability of the disorder, both genotypically and phenotypically, has led to the implication of multiple genes in the pathogenesis of WHS<sup>10</sup>. WHSC1, a protein encoded by one of several genes in the identified WHS critical region, is deleted in every known case of WHS and is dysregulated by t(4;14) translocations in lymphoid multiple myeloma<sup>11</sup>. The WHSC1 protein contains AWS-SET-PostSET domains that are highly conserved with yeast H3K36-specific methyltransferase Set2 (ref. 8) (Fig. 1a and Supplementary Fig. 1). However, the role of WHSC1 in chromatin function and its subsequent pathogenicity remain unclear.

To investigate whether WHSC1 possesses intrinsic HMTase activity, we performed *in vitro* HMTase activity assays with recombinant mouse Whsc1 (Supplementary Fig. 2a). Whsc1 preferentially methylated nucleosomal histone H3, and incorporation of histone H1 into the oligonucleosome inhibited histone methylation by Whsc1 (Fig. 1b). We determined the site specificity of Whsc1 with methylation-specific histone H3 antibodies. Whsc1 catalysed H3K36 monomethylation, dimethylation and trimethylation *in vitro* (Fig. 1c). Although

amino-terminally deleted Whsc1 proteins have been shown to methylate histones H4K20 and H3K27 (ref. 10), full-length Whsc1 did not efficiently methylate nucleosomal histones at these sites *in vitro*.

To evaluate the HMTase activity of Whsc1 in the nucleus, the Whsc1 locus was inactivated by deletion of its carboxy-terminal region, including the catalytic SET domain, in embryonic stem (ES) cells (Supplementary Fig. 3a, b). Northern blot and immunoblot analyses confirmed that no functional Whsc1 protein was expressed in homozygous Whsc1 mutant ES cells (Supplementary Fig. 3c, d). Whsc1<sup>-/-</sup> ES cells retained an undifferentiated ES-cell morphology and normal cell growth. As shown in Fig. 1d, the absence of Whsc1 did not significantly change H3K4 or H3K9 methylation. In contrast, the presence of H3K36me3, but not that of H3K36me2 or H3K36me1, was specifically decreased in Whsc1<sup>-/-</sup> ES cells. The level of H3K36me3 in Whsc1<sup>-/-</sup> ES cells was recovered when wild-type Whsc1, but not point-mutated (H1143G) inactive Whsc1 (Supplementary Figs 1 and 2b), was stably expressed in these cells (Fig. 1d).

Endogenous Whsc1 localized in the ES cell nuclei, forming several small foci that did not overlap with 4,6-diamidino-2-phenylindole (DAPI)-stained heterochromatic foci, similar to the focal staining of H3K36me3 (Fig. 1e). We found that Whsc1-containing chromatin was specifically enriched in H3K36me3, but not in H3K36me2, in comparison with the total amount of histone H3 (Fig. 1f). These results show that Whsc1 is the major HMTase to regulate histone H3K36 trimethylation selectively at euchromatic regions in ES cells.

To uncover the function of Whsc1, we immunoprecipitated Whsc1-associated proteins from ES cells stably expressing Whsc1 with a C-terminal TAP-epitope tag (Whsc1-TAP). We identified the proteins in the major bands of SDS-PAGE analysis by mass spectrometry (Fig. 2a). Immunoblotting analyses confirmed that Whsc1 associated with Sall1 (ref. 11), a member of the zinc-finger transcription factor spalt (Sal)-like protein family, O-linked N-acetylglucosamine transferase (OGT)<sup>12</sup>, and Brg1, an ATPase subunit of chromatin-remodelling complexes (Fig. 2b).

Sall1 interacts functionally with Sall4 (ref. 13), which exists as a complex with Nanog and histone deacetylase 1/2 (HDAC1/2) in ES cells<sup>14,15</sup>. Indeed, Sall4, Nanog and HDAC1, but not the ATPase subunit of the NuRD complex Mi-2, were identified as components of the Whsc1-associated proteins (Fig. 2b). We also observed a weak but significant interaction of Whsc1 with Brg1 and RNA polymerase II that was consistent with its euchromatic localization (Fig. 2b). Specific associations between Whsc1 and Sall1, Sall4 and Nanog were confirmed by co-immunoprecipitation assays (Supplementary Figs 4 and 5).

As shown in Fig. 2c, chromatin immunoprecipitation (ChIP) experiments revealed that Whsc1 localized to sites to which both

The following is a comment on the published paper shown on the preceding page.

# A Histone H3 Lysine 36 Trimethyltransferase Links Nkx2-5 to Wolf-Hirschhorn Syndrome

**NIMURA Keisuke and KANEDA Yasufumi**

(Graduate School of Medicine)

## Introduction

Deletions of human chromosome 4p16.3 cause a dominant disorder known as Wolf-Hirschhorn syndrome (WHS), which is characterized by cranio-facial malformations, mental retardation, growth delays, heart defects, and a diverse array of associated problems, many of which can be characterized as midline defects. The considerable variability of the disorder, both genotypically and phenotypically, has led to the implication of multiple genes in the pathogenesis of WHS (1). WHSC1, one of several genes in the identified WHS critical region, is deleted in every known case of WHS and is dysregulated by t(4;14) translocations in lymphoid multiple myeloma (2). The WHSC1 protein contains AWS-SET-PostSET domains that are highly conserved with yeast H3K36-specific methyltransferase Set2. However, the role of WHSC1 in chromatin function and its subsequent pathogenicity remain unclear.

## Whsc1 methylates histone H3 on lysine 36.

We performed *in vitro* HMTase activity assays using recombinant mouse Whsc1 to determine the site specificity of Whsc1 using methylation-specific histone H3 antibodies. Whsc1 catalyzed H3K36 mono-, di-, and tri-methylation *in vitro* (Fig. 1a). We next examined the HMTase activity of Whsc1 in the nucleus, the Whsc1 locus was inactivated by deletion of its C-terminal region, including the catalytic SET domain, in ES cells. The absence of Whsc1 did not significantly change H3K4 or H3K9 methylation. In contrast, the presence of H3K36me3, but not that of H3K36me2 or H3K36me1, was specifically reduced in Whsc1<sup>-/-</sup> ES cells. The level of H3K36me3 in Whsc1<sup>-/-</sup> ES cells was recovered when wild-type Whsc1, but not point-mutated (H1143G) inactive Whsc1, was stably expressed in these cells (Fig. 1b).

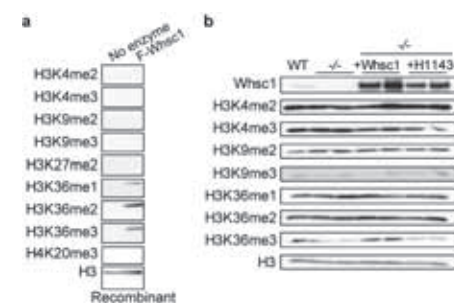


**Figure 1.** Whsc1 methylates histone H3 on lysine 36. **a**, Whsc1 catalyzes H3K36 methylation *in vitro*. Reconstituted oligonucleosomes using recombinant core histones were used as substrates for HMTase assays and analyzed by immunoblotting with the indicated specific histone H3 antibodies. **b**, Methylation status of histone H3 in wild-type or Whsc1<sup>-/-</sup> ES cells and in Whsc1<sup>-/-</sup> ES cells stably expressing either Whsc1 or mutant Whsc1 (H1143G).

## Whsc1 associates with transcription factors to repress abnormal transcription.

To uncover the function of Whsc1, we immunoprecipitated Whsc1-associated proteins from ES cells stably expressing Whsc1 with a C-terminal TAP-epitope tag (Whsc1-TAP). We identified the proteins in the major bands of SDS-PAGE analysis by mass spectrometry (Fig. 2a). Immunoblotting analyses confirmed that Whsc1 associated with Sall1, a member of the zinc finger transcription factor spalt (Sal)-like protein family, Sall4, Nanog, O-linked N-acetylglucosamine transferase (OGT), HDAC1 and Brg1, an ATPase subunit of chromatin-remodelling complexes but not the ATPase subunit of the NuRD complex Mi-2 (Fig. 2b).

Chromatin immunoprecipitation (ChIP) experiments revealed that Whsc1 localized to Nanog-Sall4 cobinding sites within the coding regions of estrogen-related receptor *Esrrb* and T-box transcription factor *Tbx3*. We found that the accumulation of H3K36me3 was significantly reduced around these Nanog-Sall4 cobinding sites in Whsc1<sup>-/-</sup> ES cells and that the levels of nuclear transcripts from these regions at *Esrrb* and *Tbx3* were increased upon deletion of Whsc1 (Fig. 2c and d).

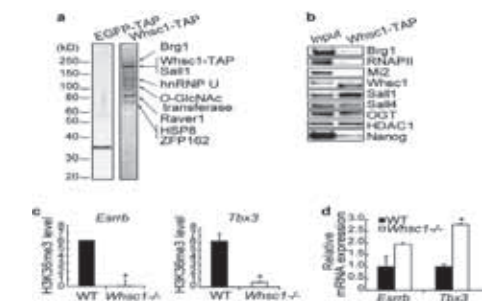


**Figure 2.** Whsc1 associates with transcription factors to repress abnormal transcription. **a**, Silver staining of Whsc1-TAP-associated proteins purified from ES cells stably expressing Whsc1-TAP. Whsc1-TAP-associated proteins as identified by mass spectrometry are indicated on the right. **b**, Purified Whsc1-TAP-associated proteins were analyzed by immunoblotting using the antibodies indicated. **c**, H3K36me3 occupancy on the *Esrrb* or *Tbx3* gene in wild-type (WT) and Whsc1<sup>-/-</sup> ES cells was analyzed by ChIP experiments. Error bars indicate SD, n = 3. **d**, Quantitative RT-PCR analysis of *Esrrb* and *Tbx3* pre-mRNA in the nucleus. Error bars indicate SD, n = 3.

## The Whsc1 gene is required for normal mouse development.

We generated Whsc1-deficient mice to elucidate the developmental and pathological role of Whsc1. Genotyping the offspring produced by interbreeding Whsc1<sup>-/-</sup> mice revealed significantly lower numbers of Whsc1<sup>-/-</sup> and Whsc1<sup>+/-</sup> mice compared to their expected Mendelian ratios at birth (Fig. 3a). The majority of Whsc1 heterozygotes survived and were fertile. However, the growth rates of Whsc1<sup>+/-</sup> mice were highly variable, and some of these mice exhibited severe growth defects,

▲Reprinted with permission from *Nature*, 460, 287-291(2009). Copyright 2009 Nature Publishing Group.

maloccluded incisors, and epicanthic folds, as seen in WHS. These results indicate that the haploinsufficiency of the *Whsc1* gene in mice causes defects as a part of WHS.

To investigate developmental defects, we stained the embryonic cartilage with alcian blue and the ossified bone with alizarin red, and found several deficiencies in midline fusion in mutant E18.5 embryos. In normal mice, the sternums fuse by E17.5 and subsequent ossification centres typically arise. *Whsc1*<sup>-/-</sup> mice did not show any ossification centres at E18.5 (Fig.3b). Even in *Whsc1*<sup>+/-</sup> mice, the appearance of ossification centres was markedly delayed. We further found incidences of cleft palate in *Whsc1*<sup>+/-</sup> mice, as is also seen in WHS.

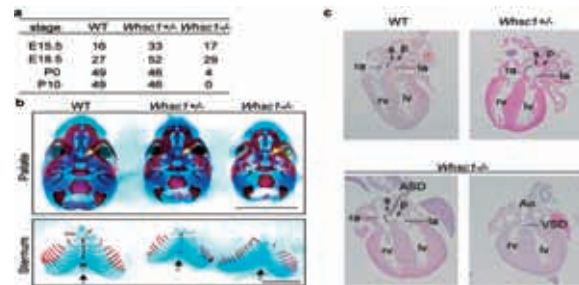


**Figure 3.** The *Whsc1* gene is required for normal mouse development. **a**, Genotype analysis of embryos and neonates from *Whsc1*<sup>+/-</sup> intercrosses. **b**, Skeletal preparation of E18.5 embryos. Cartilage was stained with alcian blue and ossified bone was stained with alizarin red. Yellow arrows, palates; black arrows, sternum. Scale bar, 5 mm. **c**, Histological analysis of *Whsc1* mutant embryonic hearts. Frontal sections from E18.5 embryos were stained with hematoxylin and eosin. Atrial septal defects (ASD) and ventricular septal defects (VSD) were observed in E18.5 *Whsc1*<sup>-/-</sup> embryos. The foramen ovals of E18.5 *Whsc1*<sup>-/-</sup> embryos were larger than those of wild-type embryos. Hypoplasia of the septum secundum was observed in E18.5 *Whsc1*<sup>-/-</sup> embryos (bracket). Ao, aortic root; lv, left ventricle; rv, right ventricle; la, left atrium; ra, right atrium; p, septum primum; s, septum secundum.

### Whsc1 is required for the appropriate transcription of *Nkx2-5*-dependent genes.

We next analyzed cardiovascular development in *Whsc1* mutant embryos, because WHS patients often have congenital heart defects, including atrial and ventricular septal defects (ASD/VSD). In wild-type mice at E18.5, the septum primum had grown to reach the atrial endocardium (Fig.3c). We found that all *Whsc1*<sup>-/-</sup> hearts showed an ASD, and half also exhibited a membranous VSD (Fig.3c, bottom). Hypoplasia of the septum secundum was observed more frequently than in wild-type mice, even in heterozygous mutant mice (Fig.3c). These results suggest that the loss of *Whsc1* causes a wide variety of midline defects, including the heart lesions seen in WHS, and leads to death after birth.

To examine whether a specific molecular interaction exists between *Whsc1* and the cardiac transcription factors, we performed coimmunoprecipitation assays using an anti-*Whsc1* antibody and found a physical interaction between *Whsc1* and a central transcriptional regulator of cardiac development, *Nkx2-5* (Fig.4a) (3). *Whsc1* and *Nkx2-5* were enriched at the first exon of *Pdgfra*, one of the up-regulated genes in *Whsc1*<sup>-/-</sup> hearts (Fig. 4b, c, d, and e).

Finally, we crossed *Whsc1*<sup>+/-</sup> and *Nkx2-5*<sup>+/-</sup> mice to investigate their functional link *in vivo*. Neither *Nkx2-5*<sup>+/-</sup> nor *Whsc1*<sup>+/-</sup> single-heterozygous mutant mice exhibited any significant defects in the septum primum or the interventricular septum of their

hearts at E18.5. In contrast, we found both an ASD and a VSD in one third of embryonic hearts from *Whsc1*<sup>+/-</sup>*Nkx2-5*<sup>+/-</sup> double-heterozygous mutants (Fig.4f). Thus, we have demonstrated here the genetic interaction between *Whsc1* and *Nkx2-5* during atrial/ventricular septal formation. Our findings partly explain that the congenital heart malformations seen in both *Whsc1* mutant mice and WHS patients are caused by dysfunction of *Nkx2-5*.

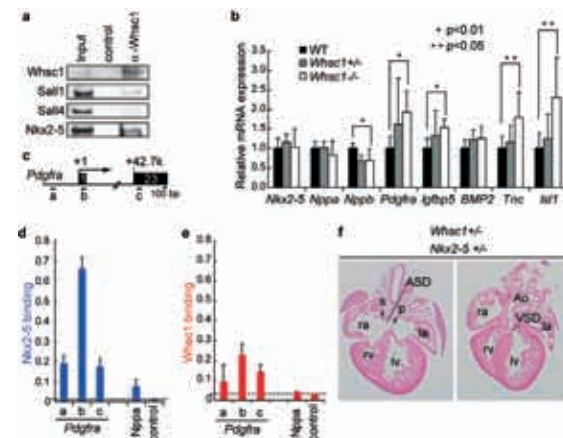


**Figure 4.** *Whsc1* is required for the appropriate transcription of *Nkx2-5*-dependent genes. **a**, *Whsc1* complex was immunoprecipitated from the nuclear extracts of E12.5 hearts using an anti-*Whsc1* or control antibody and analyzed by immunoblotting with the indicated antibodies. **b**, Quantitative RT-PCR analysis of the expressions of *Nkx2-5* and *Nkx2-5*-dependent genes. **c**, Schematic representation of the *Pdgfra* gene. Locations of genomic regions analyzed by ChIP assays are indicated. a, promoter; b, first exon; c, last exon 23. **d, e**, Native ChIP assays examining the occupancy of *Nkx2-5* (**d**) and *Whsc1* (**e**) at the *Pdgfra* regions indicated in (**c**). **f**, Histological analysis of *Whsc1*<sup>+/-</sup> and *Nkx2-5*<sup>+/-</sup> embryonic hearts. Frontal sections from E18.5 embryos were stained with hematoxylin and eosin.

### Conclusion

We have revealed a developmental and pathological link between H3K36 trimethyltransferase and transcription factors. Interactions of multiple transcription factors with *Whsc1* could account for the variability of defects caused by the *Whsc1* deficiency. Our studies provide new insights into the molecular mechanism of *Nkx2-5*-dependent gene regulation in hearts, in which *Whsc1* negatively modulates the transcriptional activity of *Nkx2-5*. Since *Nkx2-5* regulates transcription by cooperating with various cardiac transcription factors, *Whsc1* might function in the tuning of these transcriptional networks. Our findings point to a new direction for the understanding and treatment of dysregulated transcription, in which WHSC1 functions together with developmental transcription factors to prevent transcriptional pathophysiology.

### References

- [1] Bergemann, A. D., Cole, F. & Hirschhorn, K. The etiology of Wolf-Hirschhorn syndrome. *Trends Genet.* 21, 188-195 (2005).
- [2] Stec, I. et al. WHSC1, a 90 kb SET domain-containing gene, expressed in early development and homologous to a *Drosophila* dysmorphia gene maps in the Wolf-Hirschhorn syndrome critical region and is fused to IgH in t(4;14) multiple myeloma. *Hum. Mol. Genet.* 7, 1071-1082 (1998).
- [3] Prall, O. W. et al. An *Nkx2-5/Bmp2/Smad1* negative feedback loop controls heart progenitor specification and proliferation. *Cell* 128, 947-959 (2007).

## A High-Resolution Structure of the Pre-microRNA Nuclear Export Machinery

Paper in journals : this is the first page of a paper published in *Science*.

[*Science*] 326, 1275-1279 (2009)

REPORTS

## A High-Resolution Structure of the Pre-microRNA Nuclear Export Machinery

Chimari Okada,<sup>1,4\*</sup> Eiki Yamashita,<sup>1\*</sup> Soo Jae Lee,<sup>2,††</sup> Satoshi Shibata,<sup>3</sup> Jun Katahira,<sup>3,4</sup> Atsushi Nakagawa,<sup>2</sup> Yoshihiro Yoneda,<sup>3,4,5†</sup> Tomitake Tsukihara<sup>1,4†</sup>

Nuclear export of microRNAs (miRNAs) by exportin-5 (Exp-5) is an essential step in miRNA biogenesis. Here, we present the 2.9 angstrom structure of the pre-miRNA nuclear export machinery formed by pre-miRNA complexed with Exp-5 and a guanine triphosphate (GTP)-bound form of the small nuclear guanine triphosphatase (GTPase) Ran (RanGTP). The x-ray structure shows that Exp-5:RanGTP recognizes the 2-nucleotide 3' overhang structure and the double-stranded stem of the pre-miRNA. Exp-5:RanGTP shields the pre-miRNA stem from degradation in a baseball mitt-like structure where it is held by broadly distributed weak interactions, whereas a tunnel-like structure of Exp-5 interacts strongly with the 2-nucleotide 3' overhang through hydrogen bonds and ionic interactions. RNA recognition by Exp-5:RanGTP does not depend on RNA sequence, implying that Exp-5:RanGTP can recognize a variety of pre-miRNAs.

**M**ature microRNAs (miRNAs), short non-coding RNAs present in a wide range of eukaryotes (1, 2), play important roles in the regulation of biological processes including development, cell proliferation, cell differentiation, apoptosis, transposon silencing, and antiviral defense (3–6). miRNA biogenesis (7) begins in the nucleus, where capped and polyadenylated primary miRNAs, several kilobases in length, are transcribed. These are processed by the nuclear ribonuclease (RNase) III enzyme Drosha to generate ~65-nucleotide (nt) pre-miRNAs that have stem-loop structures containing 2-nt 3' overhangs. Exp-5 translocates pre-miRNAs from the nucleus to the cytoplasm through the nuclear pore complex (8–12). In the cytoplasm, the pre-

miRNAs are further processed by the cytoplasmic RNase III enzyme Dicer, which excises a ~22-base pair (bp) RNA duplex. One strand of the duplex binds to its target mRNA with imperfect complementarity, usually within the target's 3' untranslated region, assisted by the RNA-induced silencing complex (7).

Exp-5 facilitates miRNA biogenesis not only by acting as the nuclear export factor for pre-miRNAs but also by protecting pre-miRNAs from digestion by nucleases. Loss of Exp-5 results in the loss of cytoplasmic miRNA expression without nuclear accumulation of pre-miRNAs (10). Pre-miRNA binding to Exp-5 requires the guanine triphosphatase (GTPase) Ran (RanGTP). The Exp-5:RanGTP:pre-miRNA heteroternary complex formed in the nucleus is exported to the cytoplasm. Ran GTPase-activating protein, which promotes guanine triphosphate (GTP) hydrolysis in conjunction with RanBP1 and/or RanBP2, is exclusively localized in the cytoplasm and triggers the conformational change of Ran to induce release of the pre-miRNA cargo from Exp-5 (13, 14).

Here, we report the structure of the Exp-5:RanGTP:pre-miRNA complex at 2.9-Å resolution (Fig. 1A and fig. S1). This complex contains full-length human Exp-5, canine RanGTP residues 1 to 176 (removal of residues 177 to 216 stabilizes the GTP-bound conformation), and the 48-nt human pre-miRNA-30a stem domain, which includes the 2-nt 3' overhang (nucleotide

numbers 1 to 24 and 40 to 63 of human pre-miRNA-30a). Phase information used for the crystal structure analysis was derived from crystals containing Se-methionine-substituted Exp-5, and the RNA sequence was assigned from the Br anomalous signal information in crystals containing pre-miRNA 5-bromo-oxuracil derivatives. The structure was refined to an *R* factor of 0.247 and free *R* factor of 0.312, and phasing statistics are provided in table S1. We modeled 1082 of 1204 residues of Exp-5. Several loop regions in the 20 HEAT repeats and 55 residues at the C terminus could not be modeled (details in fig. S1), and 13 residues at the C terminus were modeled as a polyalanine  $\alpha$  helix. The residues 1 to 6 of Ran were not modeled because of their disordered structure. Electron density for the pre-miRNA was detected for nucleotides 1 to 11, 14 to 24, and 40 to 63 (fig. S2). The pre-miRNA-30a adopted a typical A-form RNA helical structure, 60 Å in length and 20 Å in diameter.

The Exp-5:RanGTP:pre-miRNA complex is an ellipsoid with dimensions of 65 Å by 80 Å by 110 Å. The crystal structure contains two ternary complexes, labeled A and B, in the asymmetric unit, which are essentially similar [root mean square (RMS) of 1.84 Å, where B is slightly more open than A] and present the same recognition modes for the pre-miRNA. Detailed structural comparison of ternary complexes A and B is described in (15). The structure of Exp-5 resembles a tightly wound spring, as seen in other members of the importin- $\beta$  family. Such conformations are expected to be intrinsically flexible, so small changes in the relative orientation of successive HEAT repeats could cumulatively generate substantial changes in the helical pitch (16). Ternary complex A yielded more contrast in its electron density map than did complex B; thus, all structural descriptions of the ternary complex in the following discussion will be restricted to ternary complex A. The Exp-5:RanGTP complex forms a baseball mitt-like structure in which the pre-miRNA is packed (Fig. 1B). A tunnel-like structure at the bottom of the mitt connects the inner space of the mitt with the outer space (Fig. 1B).

The pre-miRNA stem is caught in the mitt formed by the Exp-5:RanGTP complex (Fig. 1), whereas the 15-Å 2-nt 3' overhang is inserted into a tunnel formed from elements of HEAT repeats 12 to 15 (Figs. 2 and 3 and fig. S3). The inner surface of the tunnel is positively charged

www.sciencemag.org SCIENCE VOL 326 27 NOVEMBER 2009

1271

▲From *Science*, 326, Okada, C. et al., A High-Resolution Structure of the Pre-microRNA Nuclear Export Machinery, 1275-1279, 2009. Reprinted with permission from AAAS.